

Illinois State University

ISU ReD: Research and eData

Faculty publications – Physics

Physics

2-2001

Dirac theory of ring-shaped electron distributions in atoms

P Krekora

Illinois State University

R E. Wagner

Illinois State University

Q Su

Illinois State University

Rainer Grobe

Illinois State University

Follow this and additional works at: <https://ir.library.illinoisstate.edu/fpphys>



Part of the [Atomic, Molecular and Optical Physics Commons](#)

Recommended Citation

Krekora, P; Wagner, R E.; Su, Q; and Grobe, Rainer, "Dirac theory of ring-shaped electron distributions in atoms" (2001). *Faculty publications – Physics*. 31.

<https://ir.library.illinoisstate.edu/fpphys/31>

This Article is brought to you for free and open access by the Physics at ISU ReD: Research and eData. It has been accepted for inclusion in Faculty publications – Physics by an authorized administrator of ISU ReD: Research and eData. For more information, please contact ISUReD@ilstu.edu.

Dirac theory of ring-shaped electron distributions in atoms

P. Krekora, R. E. Wagner, Q. Su, and R. Grobe

Intense Laser Physics Theory Unit and Department of Physics, Illinois State University, Normal, Illinois 61790-4560

(Received 12 June 2000; published 12 January 2001)

The time-dependent Dirac equation is solved numerically on a space-time grid for an atom in a strong static magnetic field and a laser field. The resonantly induced relativistic motion of the atomic electron leads to a ringlike spatial probability density similar to the features that have been recently predicted [Wagner, Su, and Grobe, *Phys. Rev. Lett.* **84**, 3282 (2000)] based on a phase-space method. We further demonstrate that spin-orbit coupling for a fast-moving electron in such an atom becomes significant and the time dependence of the spin can dephase even if initially aligned parallel to the direction of the static magnetic field.

DOI: 10.1103/PhysRevA.63.025404

PACS number(s): 32.80.Rm, 32.60.+i

There are two main optical methods by which an atomic electron can acquire relativistic speeds. The first one involves an extremely powerful laser pulse, where the large force associated with the electric-field component of the laser is primarily responsible for accelerating the electron during a single cycle of the field. A second method to excite atoms into relativistic orbits is based on exploiting cyclotron-type resonances of the electron interacting with a combined laser and magnetic field.

Atomic resonances, however, cannot be exploited directly to bring an electron's speed up to the relativistic regime because an unlimited increase in an electron's speed at resonance is typically avoided by the nonlinearity of the atomic potential encountered by the large-amplitude motion. This limitation typically sets in at velocity scales much smaller than the speed of light. However, for an electron in a sufficiently strong magnetic field nonlinear atomic effects are not so important, and the velocity can grow to extremely large values until relativistic effects that limit the speed from growing beyond bound become important.

If the cyclotron frequency Ω associated with a static magnetic field is approximately commensurate with the laser frequency ω_L ($n\Omega \approx m\omega_L$, $n, m = 1, 2, 3, \dots$), the interaction of the electron with the combined laser and magnetic field becomes resonant. In this regime a wide variety of relativistic phenomena have been investigated recently [1]. The electronic charge distribution, for instance, can develop into ring [2], figure-8 [3], and propellerlike structures [4] whose center rotates around the nucleus. These relativistic charge-cloud distributions emerge from initial atomic states after a few laser cycles. The absence of these distributions in the corresponding nonrelativistic solution for the same parameters demonstrates that this ring structure is a genuinely relativistic phenomenon. To understand the formation of these structures, a simplified model based on the spiral orbits of individual classical trajectories was proposed which associates the relativistic dephasing with a strong velocity dispersion enhanced by the resonance between the magnetic and laser fields [1].

Until now, all theoretical predictions about these phenomena have been based on solutions to the Liouville equation for the classical phase-space density. It is thus quite crucial to determine whether these predictions can be trusted at all even qualitatively in regimes for which the nonlinearity in-

duced by the high-speed electron motion is the dominant factor for the evolution. Are intrinsic quantum-mechanical features such as interference, spin, or the discreteness of Landau levels really negligible in the relativistic regime? How well can a quantum-mechanical wave function be mimicked by a classical distribution in the nonlinear relativistic regime? Addressing these questions certainly requires an extended theory beyond classical mechanics and a full solution to the corresponding relativistic quantum system. Insight into these questions was suggested in a recent work in which for a one-dimensional harmonic oscillator the probability density from the Dirac equation turned out to be remarkably similar to the spatial density distribution from the relativistic Liouville equation despite the inherent nonlinearity due to relativity [5].

Wave-function solutions to the time-dependent Dirac equation for atoms in external fields are difficult to obtain analytically; for a few exceptions, see [6]. To overcome this technical limitation and to obtain some insights into the relativistic dynamics, numerical solutions have been studied. This computational challenge is at the forefront of computational physics and has been undertaken in the study of relativistic heavy-ion collisions [7–9] and of the interaction of atoms with intense laser fields [10–14]. The limitations due to the finite amount of CPU time and memory, even on the fastest supercomputers, are severe and restrict the accessible parameter regime that can be studied today.

However, due to recent progress in high-performance computing and in the associated software development, the dynamics of ring-shaped electron distributions can now be studied on very short time and length scales of the order of a few atomic units in two spatial dimensions (2D). Complicated by the static magnetic field, the electron motion cannot be reduced to a single spatial dimension, in which a numerical solution to the Dirac equation is feasible on even larger scales. In order to sample the initial wave function as well as the final ringlike structure on a 2D spatial grid, we had to identify a parameter regime with respect to the laser and magnetic fields such that the dynamics can develop on short time scales. The calculations described below serve more the purpose of proving the existence of quantum-mechanical ring-shaped distributions and establishing the validity of the classical mechanics approach used in Refs. [1–4] than of

simulating details of experimental situations that could be realized with today's technology.

We investigate below whether the qualitative features reported in Refs. [1–4] really hold for the fully quantum-mechanical case. By comparing the spatial phase-space density with the quantum-mechanical probability distribution we establish the validity of the classical approach. We also analyze a pure quantum effect and find that the spins can get out of phase even for an initial spin alignment that is parallel to the direction of the static magnetic field.

The classical dynamics is governed by the relativistic Liouville equation [15] (in atomic units)

$$\frac{\partial \rho(\mathbf{r}, \mathbf{p}, t)}{\partial t} = \left\{ \sqrt{c^4 + c^2[\mathbf{p} + (1/c)\mathbf{A}(\mathbf{r}, t)]^2} + V(\mathbf{r}), \rho(\mathbf{r}, \mathbf{p}, t) \right\}_{\mathbf{r}, \mathbf{p}} \quad (1)$$

for the phase-space density $\rho(\mathbf{r}, \mathbf{p}, t)$. Here $\{\dots\}_{\mathbf{r}, \mathbf{p}}$ denotes the Poisson brackets with respect to the phase-space variables, $V(\mathbf{r}) = -(\mathbf{r}^2 + 1)^{-1/2}$ is the smoothed Coulomb potential, and c is the speed of light. The vector potential $\mathbf{A}(\mathbf{r}, t) = -E_0 c / \omega_L \sin(\omega_L t - \omega_L / c y) \mathbf{e}_x + (\Omega \mathbf{e}_z) \times \mathbf{r} / 2$ represents the linearly polarized laser field along the x direction and the static magnetic field Ω is along the z direction.

Equation (1) is solved numerically via a Monte Carlo technique typically based on 50 000 particle orbits. The corresponding spatial probability distribution can be obtained via $P_{\text{cl}}(\mathbf{r}, t) \equiv \int d\mathbf{p} \rho(\mathbf{r}, \mathbf{p}, t)$. None of the phenomena discussed here are sensitive to the details of the initial state $\rho(\mathbf{r}, \mathbf{p}, t=0)$, which is chosen as $\rho(x, y, p_x, p_y, t=0) = (1/\pi^2) \exp[-(\mathbf{r}/\Delta x_0)^2/2] \exp[-2(\mathbf{p}\Delta x_0)^2]$ centered initially at the origin with a spatial width Δx_0 .

The classical distribution $P_{\text{cl}}(\mathbf{r}, t)$ will be compared directly with the corresponding quantum-mechanical density $P_{\text{qm}}(\mathbf{r}, t) = \sum_{i=1}^4 |\Psi_i(\mathbf{r}, t)|^2$, where the summation extends over the four spinor components. The wave function $\Psi(\mathbf{r}, t) = (\Psi_1, \Psi_2, \Psi_3, \Psi_4)$ can be obtained from the corresponding numerical solution to the Dirac equation:

$$i \frac{\partial}{\partial t} \Psi(\mathbf{r}, t) = \left[c \boldsymbol{\alpha} \left(\mathbf{p} + \frac{1}{c} \mathbf{A}(\mathbf{r}, t) \right) + \beta c^2 + V(\mathbf{r}) \right] \Psi(\mathbf{r}, t), \quad (2)$$

where $\boldsymbol{\alpha}$ and β denote the 4×4 Dirac matrices. The time-dependent wave function $\Psi(\mathbf{r}, t)$ can be obtained on a space-time grid using a recently developed split-operator algorithm based on a fast Fourier transformation that is accurate up to the fifth order in time [13]. In all of the simulations presented below, the two spatial axes are discretized into 65 536 grid points, which together with up to 45 000 temporal points per laser cycle lead to converged results with an overall error of less than 5%.

To have an initial quantum-mechanical state that is closest to the classical density used above we have chosen $\Psi(\mathbf{r}, t=0) = (2\pi\Delta x_0^2)^{-1/2} \exp[-(\mathbf{r}/\Delta x_0)^2/4] \Phi_{x,z}$. We used $\Phi_x = (1, -1, 0, 0)/\sqrt{2}$ and $\Phi_z = (1, 0, 0, 0)$ to represent initial states with the spins $\langle S_x(t=0) \rangle = -0.5$ a.u. and $\langle S_z(t=0) \rangle = 0.5$ a.u., respectively. The initial expectation values $[\langle x^n p_x^m \rangle_{\text{qm}} + \langle p_x^m x^n \rangle_{\text{qm}}] / 2$ for all positive integers n and m

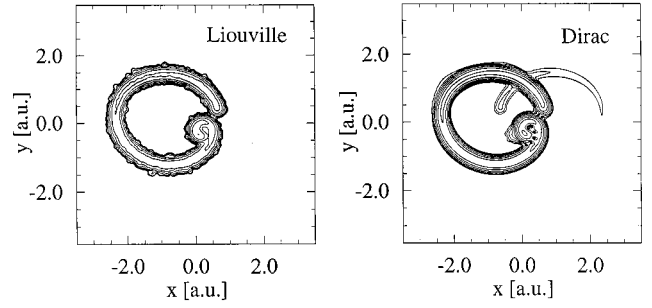


FIG. 1. Comparison of the spatial probability distributions predicted by classical and quantum mechanics. The left graph shows the solution of the relativistic Liouville equation, and the right graph is the exact solution of the Dirac equation $\sum_{i=1}^4 |\Psi_i(x, y, T)|^2$. The nine contour lines are chosen at heights $10^{-n/2}$, where $n = -1, 0, 1, \dots, 7$. (The parameters are $E_0 = 800$ a.u., $\omega_L = 80$ a.u., $\Omega = 96$ a.u., and $T = 0.66$ a.u.)

match the corresponding classical average values calculated from $\rho(\mathbf{r}, \mathbf{p}, t=0)$ via $\langle x^n p_x^m \rangle_{\text{cl}} \equiv \iint d\mathbf{r} d\mathbf{p} \rho(\mathbf{r}, \mathbf{p}, t=0) x^n p_x^m$.

In the parameter regime for which the Dirac solution is numerically feasible the electron needs to be resonantly excited within a few laser cycles. It is characterized by a cyclotron frequency $\Omega = 96$ a.u., a laser-field amplitude of $E_0 = 800$ a.u., and a frequency $\omega_L = 80$ a.u. The combined magnetic and laser field accelerates the electron to 44% of the speed of light after four laser cycles. We should note that due to the relativistic resonance shifts discussed in [1, 3, 4, 16] the maximum speed obtained in the corresponding nonrelativistic calculation is only $v = 0.33c$. This is quite counterintuitive in that relativistic effects normally lead to a less accelerated and less rapid motion that can be associated with a nonlinear mass increase.

Let us now present our results. In Fig. 1 we compare the classical with the quantum-mechanical spatial probability density after 8.4 cycles (0.66 a.u.) of the external laser force. The wave packet with an initial width $\Delta x_0 = 0.1$ a.u. develops after a few laser oscillations into a ‘‘bananalike’’ shape that evolves into a ring as shown in the figure. The center of this ring structure follows a circular orbit around the nucleus with the laser period.

Along the three lowest-density contour lines [$P < 10^{-2.5}$] in the Dirac state a ‘‘sickle’’ shape is visible that is absent in the Liouville density. This sickle can be associated with a fully developed second ring structure that is associated with the negative-energy solutions of the Dirac equation. It rotates in the opposite direction to the electron ring, as characteristic of a positive-charge cloud. The jagged contour lines at the edges of the ring (lowest densities) in the classical density are a numerical artifact due to the discreteness of the individual trajectories.

To provide a more quantitative comparison between the quantum and classical results we have displayed in Fig. 2 the effective one-dimensional probabilities obtained by integrating the total densities along the x -coordinate axis. It is clear that within the accuracies of our numerical calculations the details of classical predictions are well confirmed by the Dirac calculations. The graphs also demonstrate that the distribution along the ring is not uniform. To demonstrate that

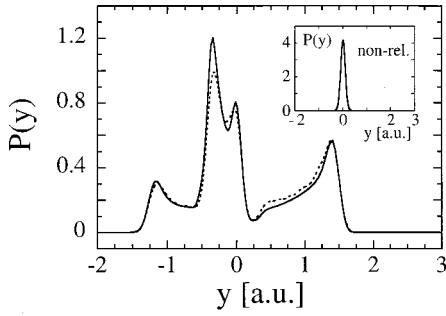


FIG. 2. The effective spatial probability along the y axis. Displayed are $\int dx \sum_{i=1}^4 |\Psi_i(x,y,T)|^2$ (continuous line) and $\iint dx dp_x dp_y \rho(x,y,p_x,p_y,T)$ (dashed line). To stress that the dynamics is fully relativistic, the inset shows the two corresponding nonrelativistic probabilities for the same parameters. (Same parameters as in Fig. 1.)

ring-shaped distributions are genuinely relativistic in nature, we display as a contrast in the inset the density obtained from the corresponding nonrelativistic calculations for the same parameters. The nonrelativistic distribution bears no similarity to the relativistic counterpart.

In Fig. 3 we present the time evolution of the expectation values for the position $\langle x(t) \rangle$ and the spatial width $\langle \Delta x(t) \rangle$. Again the classical and quantum predictions match fairly well. The maximum spatial width occurs after about seven laser cycles, which coincides with the time when the ring structure is fully developed. After this time we observe a periodic breathing pattern between the ring structure and a more localized distribution. To stress once more the fully relativistic character of the dynamics, the corresponding nonrelativistic time evolution of $\langle \Delta x(t) \rangle$ is drawn as the dotted line in Fig. 3. A nonrelativistic theory cannot explain the formation of ring-shaped electron distributions.

Let us now analyze a quantity that does not have a direct classical counterpart. For an initial state with a sharp spin value along the x direction, $\langle S_x(t=0) \rangle = -0.5$ a.u., we present in Fig. 4 the time evolution of the spin. At early times the spin precession with frequency Ω is obvious and also expected. While the electron is accelerated to relativistic

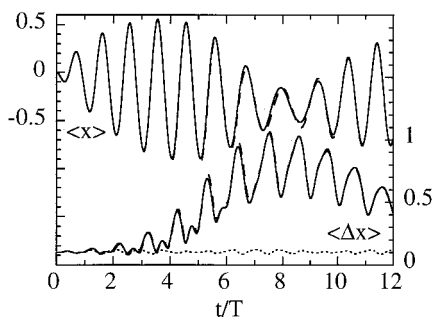
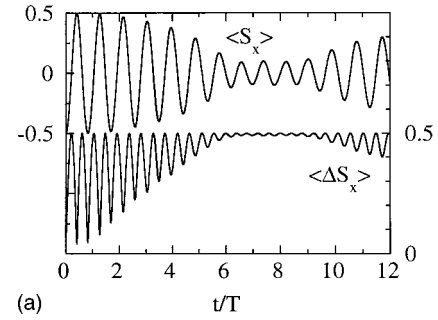
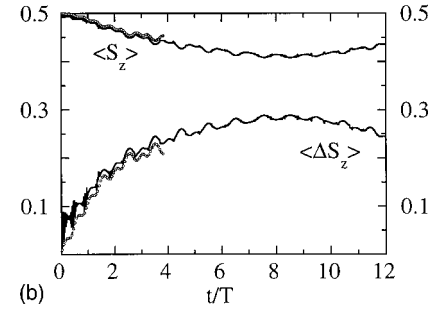


FIG. 3. Time evolution of the position $\langle x(t) \rangle$ (left axis, in a.u.) and the spatial width $\langle \Delta x(t) \rangle$ (right axis, in a.u.) according to the Dirac equation (continuous line) and the relativistic Liouville equation (dashed line). The dotted line is the (nearly constant) width according to the corresponding nonrelativistic theories. (Same parameters as in Fig. 1.)



(a)



(b)

FIG. 4. Time evolution of the spin (left axis, in a.u.) and its variance (right axis, in a.u.) for the Dirac spinor state. (Same parameters as in Fig. 1.) (a) Initial state with $\langle S_x(t=0) \rangle = -0.5$ a.u. (perpendicular to the static magnetic field); (b) initial state with $\langle S_z(t=0) \rangle = 0.5$ a.u. (parallel to the static magnetic field).

speeds, however, the spin gets out of phase, leading to a drastic reduction of the precession amplitude from 0.5 to only 0.1 a.u. after about seven laser cycles. This is a nice illustration of the fact that for relativistic speeds the time evolution of the spin cannot be viewed as independent of the orbital motion of the wave packet. We also display in Fig. 4 the variance in the spin $\langle \Delta S_x \rangle$, which takes its largest value (0.5 a.u.) when the envelope of $\langle S_x(t) \rangle$ takes its smallest value, consistent with the spin dephasing. All expectation values are averages computed from the total quantum state. By (arbitrarily) dividing the wave function into different spatial sectors, we find that the spin alignment depends on the position. In the future we plan to investigate the time evolution of the spatial spin distribution in more detail [17].

We should mention that the same type of spin dephasing can be observed even parallel to the static-magnetic-field direction. Figure 4(b) shows this effect for an initial eigenstate of S_z . The spin $\langle S_z(t) \rangle$ decays from 0.5 to 0.4 a.u. in a more or less monotonic fashion. The early-time behavior in $\langle S_z(t) \rangle$ and $\langle \Delta S_z(t) \rangle$ can be crudely mimicked if we approximate the state by a (field-free) positive-energy eigenstate with an average square velocity $\langle \mathbf{v}^2 \rangle$. This assumption leads to the expression $\langle S_z(t) \rangle = \frac{1}{2} \sqrt{1 - [\langle \mathbf{v}(t) \rangle / c]^2}$. This prediction and the corresponding one for $\langle \Delta S_z \rangle$ are represented by the circles in Fig. 4(b), where $\langle \mathbf{v}^2(t) \rangle$ is calculated from the numerical data for $\langle x(t) \rangle$ and $\langle y(t) \rangle$ similar to these presented in Fig. 3.

The graphs in Fig. 4 are essentially unchanged if the laser-field coupling is evaluated in the dipole approximation. This suggests that the oscillating magnetic-field component of the electromagnetic radiation pulse is not relevant for the

unexpected spin dephasing. We have also recalculated the orbital data leading to Figs. 2 and 3 but for an initial state with $\langle S_z(t=0) \rangle = 0.5$ a.u. The spatial data for $\langle x(t) \rangle$ and $\langle \Delta x(t) \rangle$ differed by less than 5% from those with a different initial spin state. This difference is too close to our numerical error to allow for a definite conclusion about how the spin affects the orbital motion.

In summary, we have shown that the predictions of ring-shaped electron distributions based on classical mechanics are confirmed by the Dirac theory. A direct comparison of the quantum expectation values of the position and spatial width with the classical counterparts does not reveal any ma-

nor difference in the relativistic domain. Furthermore, this resonance regime reveals a spin-dephasing effect that may be associated with the coupling between the spin and the orbital motion.

This work was supported by the NSF under Grant No. PHY-9970490. We also acknowledge support from the Research Corporation for Cottrell Science Awards and ISU for URGs. R.E.W. thanks the Illinois State University Undergraduate Honors Program for support of his research work. The numerical work was performed at NCSA.

-
- [1] Sci. News (Washington, D. C.) **157**, 287 (2000); R. E. Wagner, Q. Su, and R. Grobe, Phys. Rev. Lett. **84**, 3282 (2000).
 - [2] For movies of ring-shaped electron distributions see Phys. Rev. Focus **5**, story 15, 6 April 2000 at the web site <http://focus.aps.org/v5/st15.html> story
 - [3] P. J. Peverly, R. E. Wagner, Q. Su, and R. Grobe, Laser Phys. **10**, 303 (2000).
 - [4] Q. Su, R. E. Wagner, P. J. Peverly, and R. Grobe, in *Frontiers of Laser Physics and Quantum Optics*, edited by Z. Xu, S. Xie, S.-Y. Zhu, and M. O. Scully (Springer, Berlin, 2000), p. 117.
 - [5] R. E. Wagner, P. J. Peverly, Q. Su, and R. Grobe, Phys. Rev. A **61**, 35 402 (2000).
 - [6] V. G. Bagrov and D. M. Gitman, *Exact Solutions of Relativistic Wave Equations* (Kluwer, Dordrecht, 1990).
 - [7] C. Bottcher and M. R. Strayer, Ann. Phys. (N.Y.) **175**, 64 (1987).
 - [8] J. C. Wells, A. S. Umar, V. E. Oberacker, C. Bottcher, M. R. Strayer, J.-S. Wu, J. Drake, and R. Flanery, Int. J. Mod. Phys. C **4**, 459 (1993).
 - [9] K. Momberger, A. Belkacem, and A. H. Sorensen, Phys. Rev. A **53**, 1605 (1996).
 - [10] U. W. Rathe, C. H. Keitel, M. Protopapas, and P. L. Knight, J. Phys. B **30**, L531 (1997).
 - [11] N. J. Kylstra, A. M. Ermolaev, and C. J. Joachain, J. Phys. B **30**, L449 (1997).
 - [12] C. Szymanowski, C. H. Keitel, and A. Maquet, Laser Phys. **9**, 133 (1999).
 - [13] J. W. Braun, Q. Su, and R. Grobe, Phys. Rev. A **59**, 604 (1999).
 - [14] U. W. Rathe, P. Sanders, and P. L. Knight, Parallel Comput. **25**, 525 (1999).
 - [15] H. Goldstein, *Classical Mechanics*, 2nd ed. (Addison-Wesley, New York, 1980).
 - [16] R. E. Wagner, Q. Su, and R. Grobe, Phys. Rev. A **60**, 3233 (1999).
 - [17] P. Krekora, Q. Su, and R. Grobe (unpublished).